Journal of Zhejiang University-SCIENCE A (Applied Physics & Engineering) *2024 25(1):36-46*
www.jzus.zju.edu.cn; www.springer.com/journal/11582
E-mail: jzus_a@zju.edu.cn

Research Article
https://doi.org/10.1631/jzus.A2300006

Check for updates

Biotreatment of incinerated bottom ash and biocementation of sand blocks using soybean urease

Xiaoniu YU[1], Yidong XU[2]✉

[1]*Jiangsu Key Laboratory of Construction Materials, Southeast University, Nanjing 211189, China*
[2]*School of Civil Engineering and Architecture, NingboTech University, Ningbo 315100, China*

Abstract: Because of the high cost of cultivating urease-producing bacteria (UPB), this paper proposes soybean-urease-induced carbonate precipitation (SUICP) as a novel biocement for treatment of nickel contaminants and cementation of sandy soil. We found the optimal soaking time and soybean-powder content to be 30 min and 130 g/L, respectively, based on a standard of 5 U of urease activity. The most efficient removal of nickel ions is obtained with an ideal mass ratio of urea to nickel ions to soybean-powder filtrate (SPF) of 1:2.4:20. The removal efficiency of nickel ions can reach 89.42% when treating 1 L of nickel-ion solution (1200 mg/L with the optimal mass ratio). In incinerated bottom ash (IBA), the removal efficiency of nickel ions is 99.33% with the optimal mass ratio. In biocemented sandy soil, the average unconfined compressive strength (UCS) of sand blocks cemented with soybean urease-based biocement can reach 118.89 kPa when the cementation level is 3. Currently, the average content of $CaCO_3$ in sand blocks is 2.52%. As a result, the SUICP process can be applied to remove heavy metal ions in wastewater or solid waste and improve the mechanical properties of soft soil foundations.

Key words: Biocement; Soybean-powder filtrate (SPF); Removal efficiency; Sandy soil; Unconfined compressive strength (UCS)

1 Introduction

Microbial-induced carbonate-precipitation (MICP) cement is widely used in the field of civil and environmental engineering (DeJong et al., 2006; Liu et al., 2021; Lv et al., 2022; Qian et al., 2022; Xiao et al., 2022; Xue et al., 2022; Zhang et al., 2022; Yu and Zhang, 2023b). It can reinforce sandy soil foundations and repair cracks in cement-based and rock materials for civil engineering applications (Jiang et al., 2020; Li et al., 2020; Lin et al., 2020; van der Bergh et al., 2020; Fan et al., 2023; Kou et al., 2023). In the field of environmental engineering, MICP cement can remove heavy metal ions in soil, water, and solid waste (Li et al., 2010; Jiang et al., 2019; Yin et al., 2021; Song et al., 2022). The most commonly used MICP cement involves urease-producing bacteria (UPB), which can hydrolyze urea to produce carbonate ions that react with surrounding calcium ions to form calcium carbonate with cementing properties (Xiao P et al., 2018; Hoang et al., 2020, 2023; Gebru et al., 2021; Xiao Y et al., 2021; Wu et al., 2023). UPB can be isolated from limestone caves and carbide slag (Omoregie et al., 2016; Wu et al., 2020), and enlarged for production for in-situ soil biocementation (Omoregie et al., 2020). MICP cement is similar to ordinary Portland cement (OPC); it can consolidate loose sandy soil particles and repair cracks in cement-based materials (Cheng et al., 2014; Meng et al., 2021; Sun et al., 2021; Xiao et al., 2023; Yu and Zhang, 2023a). Seawater-based UPB and cementation solution can be applied to bind sea sand and sandy soil, and their permeability and compressive strength are successfully improved in marine environments (Cheng et al., 2014; Yu and Rong, 2022). The erosion of sand-soil slopes by seawater, river water, or rainwater can be effectively controlled using MICP cement, as demonstrated by Kou et al. (2020), Sun et al. (2022), and Xiao et al. (2022). Furthermore, the use of biocementation has significantly enhanced the anti-landslide performance of these slopes. These studies provide strong evidence that MICP cement is a

✉ Yidong XU, xyd@nit.zju.edu.cn
Xiaoniu YU, https://orcid.org/0000-0002-1386-9966
Yidong XU, https://orcid.org/0000-0003-3756-032X

Received Jan. 5, 2023; Revision accepted Apr. 14, 2023;
Crosschecked Sept. 19, 2023

© Zhejiang University Press 2024

valuable asset in the field of civil and environmental engineering. Due to the need for specialized cultivation during the production of biocement using UPB, large-scale application in practical engineering may not be feasible.

Soybeans can be grown on a large scale, with a growth cycle of approximately five months, and the yield in China is approximately 1800 kg/ha. Soybeans are rich in a variety of nutrients that can enhance immunity and improve diet (He and Chen, 2013; Nile et al., 2020). The protein content of soybeans is about 36.5%, including soybean urease protein (He and Chen, 2013; Nile et al., 2020). Soybean urease is soluble in water, alcohol, and acetone, which means that these solvents can be used to extract it. The activity of soybean urease in hydrolyzing urea to produce carbonate ions is similar to, but more easily controllable than, that of microbial urease. The carbonate ions react with surrounding calcium ions to produce calcium carbonate, which serves as a cementing agent. This process is called soybean-urease-induced carbonate precipitation (SUICP), and is similar to MICP (Lee and Kim, 2020; Fan et al., 2022; Garg et al., 2023).

Soybean-urease-based biocements such as those produced by SUICP process can bind loose sand particles and repair cracks in cement-based materials and rock. Unlike UPB, soybeans do not require professional cultivation, which can save costs (Gao et al., 2019; Xiao et al., 2019). The price of soybeans is much lower than that of commercially available pure plant-based urease, which is in turn lower than that of UPB. Thus, soybean urease is advantageous because it is non-toxic, inexpensive, and eco-friendly (Moghal et al., 2020). The urease can be extracted from soybean powder by soaking it in an aqueous solution, and the process is simple and fast compared with the preparation of UPB solution. Therefore, soybean-urease-based biocement has broad application prospects for biocementation of sandy soil and biotreatment of heavy metals. The soybean-powder filtrate (SPF) has a certain level of viscosity that may affect cementation levels, and thus the soil-reinforcement effect. Therefore, it is necessary to find a way to extract high-purity soybean urease.

To extract urease, soybeans are ground into a fine powder and then soaked in deionized (DI) water. Urease activity resulting from different soaking times and soybean-powder content is measured based on changes in conductivity. The optimal soaking time and concentration of SPF are determined through a combination of urease activity and cost. The SPF is then used to remove nickel ions from the solution and incinerated bottom ash (IBA). Optimal removal conditions are determined by adjusting reaction time, urea content, and SPF concentration. By attending to all these factors, different concentrations of nickel ions can be removed well from solution and IBA. Loose sand particles can also be cemented into a whole with better mechanical performance by soybean-urease-based biocement with the optimal SPF concentration. In this way, soybean-urease-based biocement can be used to replace MICP cement and OPC in the cementation of sandy soil and treatment of waste solids containing heavy metals.

2 Materials and methods

2.1 Materials

Nickel (II) chloride hexahydrate ($NiCl_2·6H_2O$, analytical reagent) was used to prepare nickel-ion solutions, and was configured with a concentration of 1200 mg/L. The soybeans were purchased from a nearby supermarket and were imported from Canada. The price of the beans was approximately 770 USD/t. We ground the soybeans into powders of different fineness with a pulverizer (Fig. S1 of the electronic supplementary materials (ESM)). The various powders were sealed and refrigerated at low temperatures before use. The IBA contained heavy metals obtained from city landfills, as shown in Fig. S2a. The particles had an irregular block-like structure with a rough surface (Fig. S2b). The nickel-ion content was (197.09±2.41) mg/kg, as determined from the IBA with an inductively coupled plasma emission spectrometer (ICP-OES, Optima 8000, PerkinElmer, USA). The nickel-ion content eluted from the IBA was (0.060±0.005) mg/kg. The amount of 1 mol of the mixture of urea and calcium chloride dihydrate was dissolved in 1 L of DI water to obtain a cementation solution of 1 mol/L.

2.2 Extracting urease from soybean powder

The 10 g of soybean powder was mixed with 100 mL of DI water and soaked for 10, 30, 50, 70, 90, or 120 min (Table S1) (Yu and Pan, 2023). The SPF was obtained by filtering through four layers of gauze with an aperture size of approximately 1 mm. The SPF

(2 mL) was thoroughly mixed with a urea solution of 10 mL (3 mol/L) and DI water of 8 mL in a plastic tube. The change in its conductivity was measured over 1 min to determine urease activity.

The soybean powders (1, 3, 5, 7, 10, 13, and 15 g) were mixed with 100 mL of DI water and soaked for 30 min, as shown in Table S2 (Yu and Pan, 2023). The SPFs of different concentrations were obtained via filtering through four layers of gauze. We then observed and determined the change in the conductivity for each concentration.

2.3 Preparation of bio-carbonate minerals

The nickel-ion solution (100 mL, 1200 mg/L) was put in a beaker. Based on the optimal quality ratio of urea to nickel ions to SPF (1:2.4:20), we added 50 mg of urea and 1000 mg of SPF to the nickel-ion solution, mixed them evenly, and stilled the resulting solution at room temperature (26 ℃) for 24 h. We then obtained precipitates by filtering the solution. Samples were washed with tap water three times and finally dried in an oven. The flowchart for the biotreatment of IBA is shown in Fig. 1.

The cementation solution (50 mL, 1 mol/L) was put into a beaker. Next, 50 mL of SPF was added to the above cementation solutions, mixed thoroughly, and stilled at room temperature (26 ℃) for 24 h. The microstructure of synthesized bio-carbonate cement is similar to the carbonate produced in the process of biocementation of sandy soil. Fig. 2 shows the flowchart for biocementation of sand blocks. All samples were washed with tap water three times. After drying the samples, we collected bio-carbonate minerals by lightly grinding the sand blocks.

2.4 Mineralization and removal of nickel ions

2.4.1 Removal of nickel ions under different conditions

Urea (110 mg) was dissolved in each of seven identical nickel-ion solutions (10 mL, 1200 mg/L). Then 1 mL of SPF (130 g/L) was added and mixed well and the solution was stilled for 0, 2, 4, 6, 8, 24, 48, or 72 h (Table S3).

Urea (110 mg) was also dissolved into five identical nickel-ion solutions (10 mL, 1200 mg/L). Then 0.2, 0.5, 1.0, 1.5, or 2.0 mL of SPF (130 g/L) was added, shaken well, and stilled for 24 h, as shown in Table S4.

Different amounts of urea (10, 30, 50, 70, 90, 110, 130, and 150 mg) were dissolved into eight identical nickel-ion solutions (10 mL, 1200 mg/L). SPF (1 mL, 130 g/L) was added into each solution, shaken well, and stilled for 24 h (Table S5).

After 24 h, clear light blue solutions were obtained by passing liquids through a paper filter.

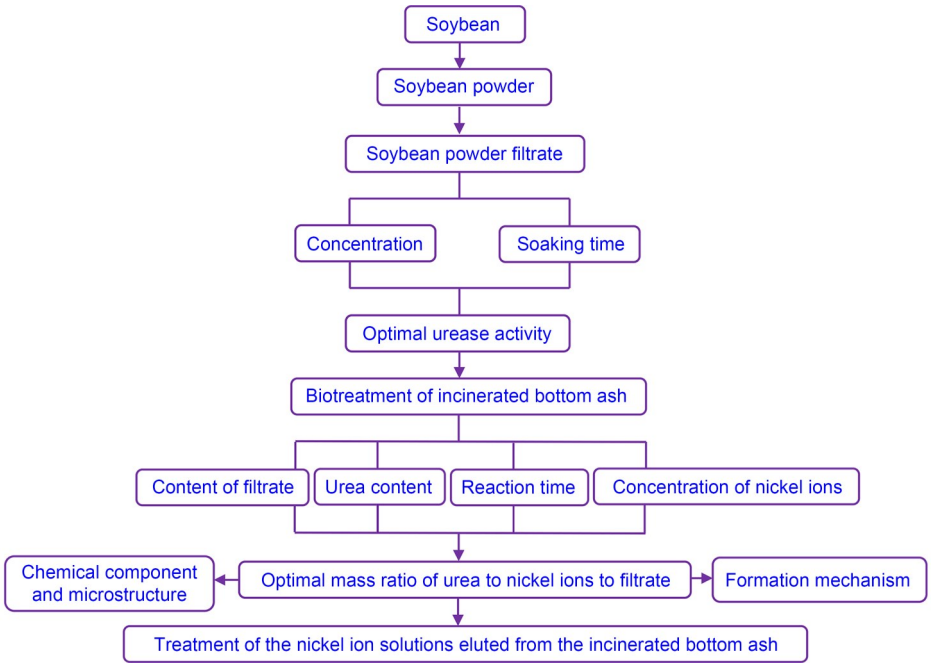

Fig. 1 IBA biotreatment flowchart

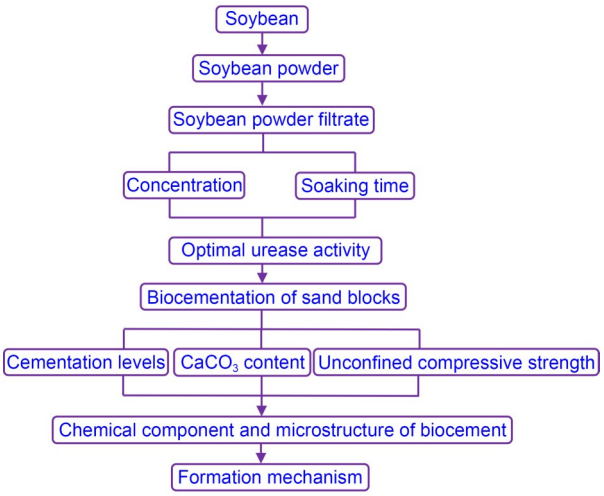

Fig. 2 Sand-block biocementation flowchart

2.4.2 Removal of different concentrations of nickel ions in solution under optimal conditions

The four groups of 20 mL of nickel-ion solution (120, 600, 1200, and 3000 mg/L) were taken out and put into beakers. Based on the optimal mass ratio of urea to nickel ions to SPF (1:2.4:20), we added the corresponding mass of urea and SPF to the solution and mixed it thoroughly at room temperature (26 ℃) for 24 h, as shown in Table S6. After 24 h, clear light blue solutions were obtained by passing the liquids through a paper filter.

2.4.3 Removal of different amounts of nickel ions in the IBA under optimal conditions

The content of nickel ions was adjusted in the IBA to simulate the actual concentration of nickel pollution in the environment. The contents of nickel ions per kilogram of IBA were 120.03, 600.03, and 1200.03 mg. The DI water (1 L) was added into the IBA with different nickel-ion contents. The solution of 100 mL was taken out and put in a beaker. Based on the optimal mass ratio of urea to nickel ions to SPF (1:2.4:20), we added the corresponding masses of urea and SPF and mixed them evenly. All samples were stilled at room temperature (26 ℃) for 24 h (Table S7). After 24 h, clear solutions were obtained by passing the liquids through a paper filter.

2.5 Biocemented sand blocks

Ottawa sand weighing 215 g (20/30 meshes) was put in a cube model. First, 50 mL of SPF (130 g/L) was poured into sand blocks (50 mm×50 mm×50 mm), and the specimens were then set for 15 min. Next, 50 mL of cementation solution (1 mol/L) was added to the blocks and then left for 24 h. Each group contained three samples. The cementation levels were 1, 2, and 3. All specimens were washed three times with tap water. We then measured the unconfined compressive strength (UCS) and calcium carbonate content of the sand blocks using an electronic testing machine set at 1 mm/min and 2 mol/L hydrochloric acid (HCl) (Yu and Rong, 2022).

2.6 Characterization of samples

2.6.1 Determination of urease activity

The SPF (2 mL) was mixed with 10 mL of urea (3 mol/L) and 8 mL of DI water in 25 mL of the plastic tube (Yu and Rong, 2022). A conductivity probe (Orion Star A212 Conductivity Meter, Thermo Fisher Scientific Inc., USA) was put into the mixed solution to record the change in conductivity. Based on the conductivity change over 1 min, we calculated the urease activity using Eq. (1) (Whiffin et al., 2007; Cheng et al., 2017; Yu and Rong, 2022):

$$U = S \times 11.11 \times 10, \tag{1}$$

where U is the urease activity, μmol/min, and S is the conductivity, mS.

2.6.2 Powder X-ray diffraction (XRD) analysis

Bio-carbonate minerals were put in a sample tank. The specimens were scanned at a speed of 2.5 (°)/min, 2θ ranging from 5° to 80° and λ=1.5406 Å by powder X-ray diffraction analysis (XRD, Bruker D8-Advance, Bruker Company, Germany). Chemical components of bio-carbonate minerals were determined by indexing raw files produced by XRD equipment with MDI Jade 5.0.

2.6.3 Field emission scanning electron microscopy with energy-dispersive X-ray spectroscopy (FESEM-EDS)

First, we sprayed the surface of the samples with a layer of platinum in a vacuum environment. Next, we placed them into the sample compartment of the FESEM analyzer (JSM-7600F, JEOL, Japan). We adjusted the acceleration voltage of the electron gun to 5.0 kV, and were able to determine the morphology and size of nickel carbonate and sand blocks from the FESEM images and record their elemental compositions with EDS.

2.6.4 Unconfined compressive strength (UCS)

The UCS of sand blocks was determined with an electronic testing machine (DDL 100, Sinotest Equipment Co., Ltd., China). The axial load was applied at a constant rate of 1.0 mm/min (Yu and Rong, 2022), and UCS values were recorded in triplicate.

3 Results and discussion

3.1 Effects of soaking time and soybean-powder content on urease activity

The effect of soaking time on urease activity has been reported by Yu and Pan (2023). The urease activity of 5 U and soybean cost are used to determine the optimal content of SPF. When the urease activity in SPF is greater than 5 U, it can better remove heavy metals and cement sandy soil (Cheng et al., 2017). The average urease activity is higher than 5 U when the soaking time is 30, 70, 90, or 120 min (Yu and Pan, 2023), and the optimal soaking time appears to be 30 min. At a soaking time of 30 min, the average urease activity increases with the increase of the concentration of SPF (Yu and Pan, 2023). Yu and Pan (2023) found that the optimal concentration of SPF in terms of soybean cost is 130 g/L. Therefore, the optimal soaking time and concentration of SPF are 30 min and 130 g/L, respectively (Yu and Pan, 2023).

3.2 Chemical components and microstructures of bio-carbonate minerals

EDS images show that the elements C, O, Ni or C, O, and Ca distributed widely over the entire figure (Figs. S3 and S4). Three elements overlap. Nickel- and calcium-carbonate-type compounds are determined from element overlap. Fig. 3 shows that a nickel- or calcium-carbonate-type compound can be precipitated by the SUICP process. Hence, nickel ions can react with carbonate ions to form water-insoluble nickel hydroxide carbonate ($Ni_2CO_3(OH)_2{\cdot}H_2O$) (Do et al., 2020), which can remove nickel ions from wastewater and solid waste (Fig. 3a). In sand particles, calcium ions react with carbonate ions to produce calcite ($CaCO_3$, calcite) with cementing properties and can act as a bridge to connect sand particles, as a result of having certain mechanical properties (Gebru et al., 2021; Yi et al., 2021; Gao et al., 2022) (Fig. 3b). The soybean-urease-based biocement can be used for soil improvement and solid-waste treatment.

Fig. 4a displays FESEM images of nickel-carbonate-type compounds precipitated by the SUICP process. The morphology and size of the nickel hydroxide carbonate are evident in the FESEM images. The

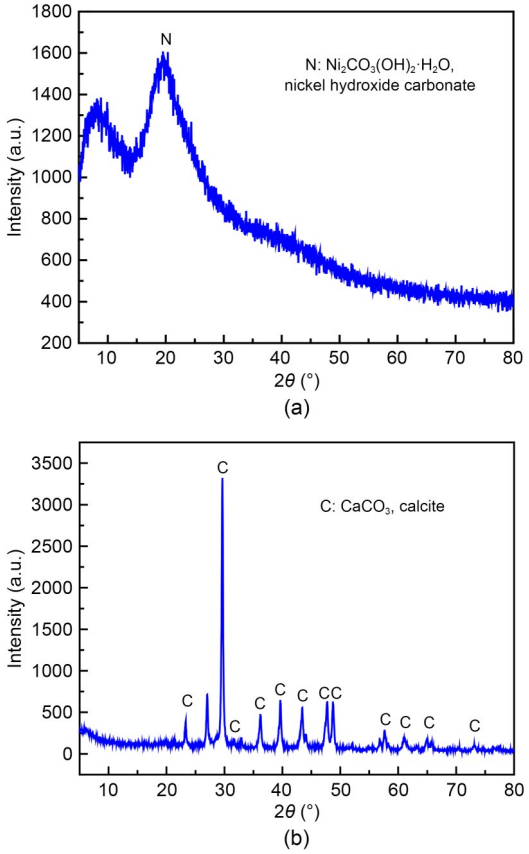

Fig. 3 XRD patterns of nickel hydroxide carbonate (a) and calcite (b) precipitated by the SUICP process

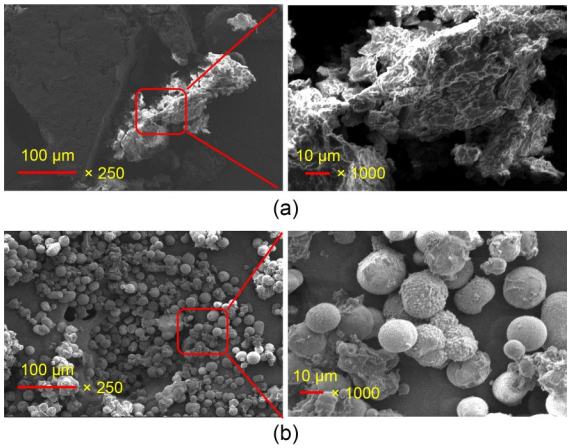

Fig. 4 FESEM images of nickel hydroxide carbonate (a) and calcite (b) precipitated by the SUICP process

morphology of the nickel-carbonate-type compound is an irregular block structure with particle size below 200 μm. The shape and diameter of the calcite are shown in Fig. 4b. The microstructure of calcite is regular and irregular spheres with a size range of 5–50 μm, and regular and irregular spheres of calcite can be filled into pores of sandy soil and bind them together (Yu and Rong, 2022). The soybean-urease-based biocement can be used in the field of civil and environmental engineering according to the formation mechanism.

3.3 Effects of SPF content, urea content, reaction time, and nickel-ion concentration on removal efficiency of nickel ions

We used a nickel-ion solution of 10 mL with an initial concentration of 1200 mg/L. The concentration of the SPF was 130 g/L. The effects of SPF concentration, urea content, and reaction time on the removal efficiency of nickel ions are shown in Fig. 5. All samples were kept still in the experimental room for 0–24 h. After 24 h, the removal efficiency of nickel ions increased with the increase of reaction time, but the degree of increase was small. Therefore, the optimal reaction time appeared to be 24 h (Fig. 5a). When the content of SPF was 1 or 2 mL, the removal efficiency of nickel ions was higher than those for other content levels. The removal efficiency of nickel ions for an SPF content of 2 mL was slightly higher than that for 1 mL of SPF. The optimal SPF content was selected as 1 mL (approximately 1000 mg), as shown in Fig. 5b. With the optimal reaction time and SPF content, the optimal urea mass was 50 mg. Under those conditions, the nickel-ion and urea contents were 120 and 50 mg, respectively (Fig. 5c). Therefore, the optimal mass ratio of urea to nickel ions to SPF is 1:2.4:20 when the concentration of SPF is 130 g/L. The removal efficiency of nickel ions is approximately 90% with the SUICP process, which is higher than that of microbial-induced phosphate precipitation (MIPP) under optimal conditions (Yu and Jiang, 2019).

The pH of nickel-ion solutions is approximately 5 at concentrations of 120, 600, 1200, and 3000 mg/L,

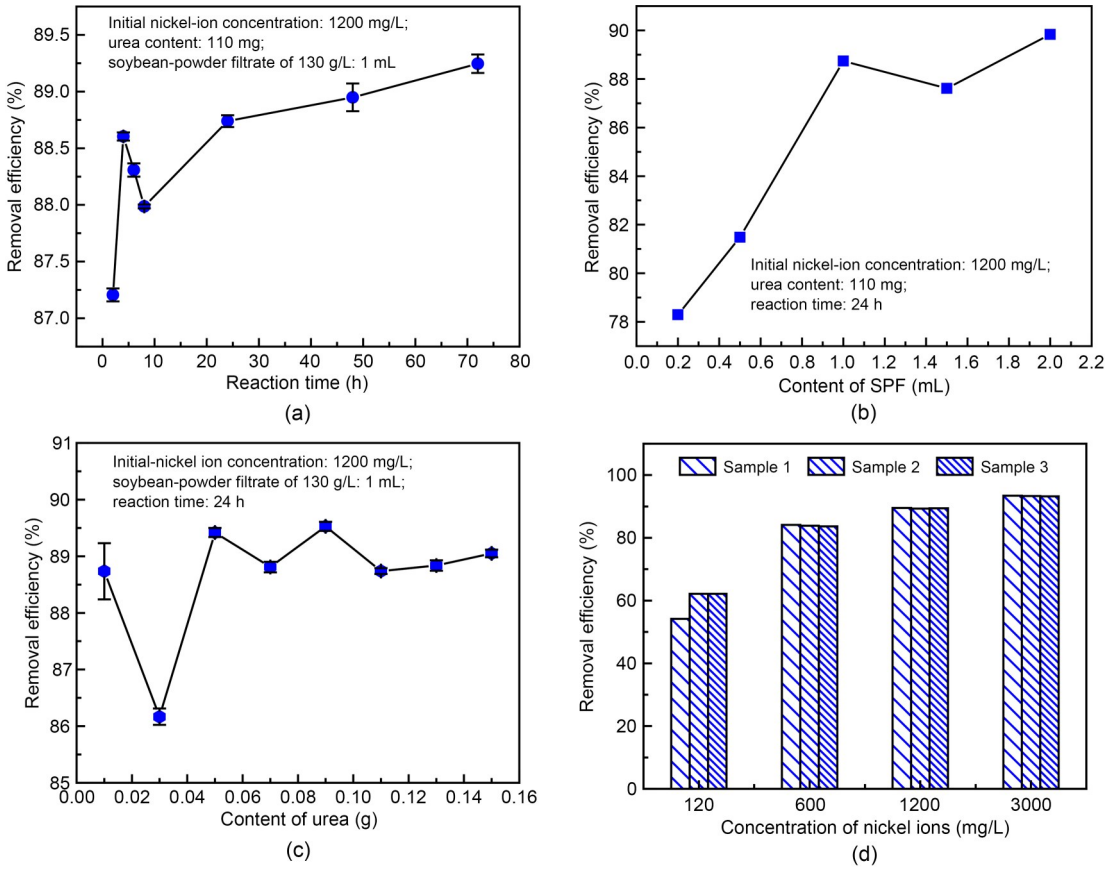

Fig. 5 Influence of reaction time (a), SPF content (b), urea content (c), and concentration of nickel ions (d) on removal efficiency of nickel ions

which indicates weak acidity. The average removal efficiencies of nickel ions are 59.50%, 83.87%, 89.42%, and 93.25% when the concentrations of nickel ions are 120, 600, 1200, and 3000 mg/L, respectively, with the optimal mass ratio of urea to nickel ions to SPF (1:2.4:20), as shown in Fig. 5d. Samples 1, 2, and 3 belonged to one group of specimens. The experimental results show that the removal efficiency increases as the concentration of nickel ions increases. The solubility product constant of nickel carbonate (1.42×10^{-7}) demonstrates that high concentrations of carbonate and nickel ions are conducive to a shift of the reaction equilibrium to the formation of nickel carbonate with the same volume. Hence, when the concentration of nickel ions is higher, the removal efficiency is better. In electroplating wastewater, the removal efficiency of nickel ions at 1475 mg/L can reach above 90% with the SUICP process, which is better than the removal rate with phosphate microbial mineralization (Yu and Jiang, 2019). Therefore, the SUICP process can be advantageously applied to remove nickel ions from electroplating wastewater.

3.4 Treatment of nickel-ion solutions eluted from IBA

Fig. 6 shows the removal efficiency for different amounts of nickel ions in IBA. The pH of the solution eluted from the IBA was approximately 11 when the mass ratio of water to IBA was 2:1. The concentrations of nickel ions in the solution eluted per kilogram of IBA were 120.03, 600.03, and 1200.03 mg/L, respectively. Samples 1, 2, and 3 belong to the same group of specimens. With the optimal mass ratio of urea to nickel ions to SPF, the average removal efficiencies of nickel ions can reach 98.79%, 99.33%, and 94.77% when the nickel ion concentration was 120.03, 600.03, and 1200.03 mg/L, respectively. The experimental results show that different amounts of nickel ions eluted from IBA can be removed well, with an efficiency of up to 94%. A comparison of the removal efficiency for different concentrations of nickel ions in the eluted solution shows that alkaline IBA is beneficial for the removal of nickel ions by the SUICP process.

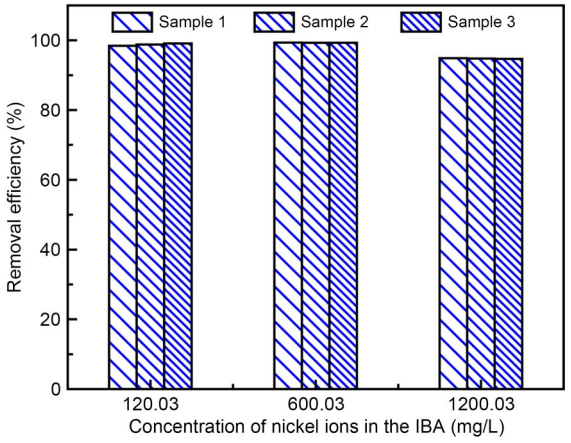

Fig. 6 Removal efficiency of different levels of nickel-ion content from IBA

3.5 Biocementing sand blocks using SUICP

Loose sand blocks (50 mm×50 mm×50 mm) can be cemented into a whole through the SUICP process, as shown in Fig. 7a. Each group of blocks contained three samples. The UCS of sand blocks was determined by a 1.0 mm/min electronic testing machine under wet conditions. The average UCS values were 2.52, 24.85, and 118.88 kPa at cementation levels of 1, 2, and 3, respectively (Fig. 7b). When the cementation level was higher than 3, the soybean-urease-based biocement could be used to improve the bearing capacity of the sand foundation. As shown in Fig. 7c, the $CaCO_3$ content of sand blocks increased with the increase of cementation level. The $CaCO_3$ content was determined by the acid dissolution method until no air bubbles were generated in the sand blocks. They were left to stand for 2 h and then dried in an oven to determine the mass before and after. Finally, we obtained the $CaCO_3$ content of the sand blocks. The average $CaCO_3$ content was 1.81%, 2.51%, and 2.52% when the cementation level was 1, 2, and 3, respectively. The urease extracted from Chinese soybeans can also be used to hydrolyze urea and bind sandy soil (Shu et al., 2022). Its cementation effect is similar to that of Canadian soybean urease when used on the sand with similar $CaCO_3$ content (Shu et al., 2022). When the cementation level is higher than 1, it is difficult to pour SPF sand blocks manually. When the level is higher than 3, a peristaltic pump should be used to inject the soybean-urease-based biocement into sand blocks; a higher UCS can then be obtained. Pores of sand blocks are filled well by biocement, and this increases cementation levels (Yu and Pan, 2023). The UCS of sand blocks increases as the cementation level rises (Yu and Rong, 2022). Because the cementation level increases with the content of biocement, this content is proportional to UCS in the sand.

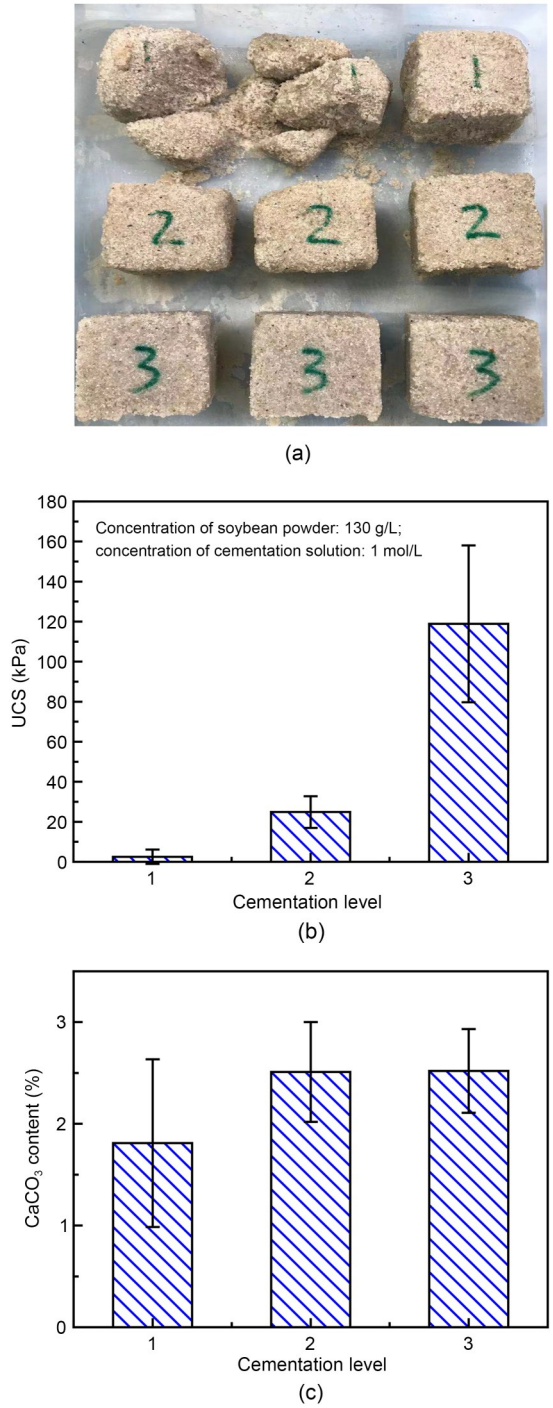

Fig. 7 Cementation state (a), UCS (b), and $CaCO_3$ content (c) of biocemented sand blocks

3.6 Potential applications and formation mechanism of soybean-urease-based biocement

Soybean-urease-based biocement can be applied to remove heavy metals, as well as to bind sand blocks. As explained above, soybeans contain a certain amount of urease, which can be dissolved in water, ethanol, acetone or their mixed solution (Fig. S5). Soybean-based urease has the same function as microbial urease; it can hydrolyze urea to produce carbonate and ammonium ions, as shown in Fig. 8 (Yu et al., 2022; Yu and Pan, 2023). The Ni(I) in soybean-based urease is coordinated with urea to form a urease-urea complex (Benini et al., 2001). The urease-urea complex forms urease, carbamate, and ammonia after structural transformation and proton transfer (Benini et al., 2001). In an aqueous solution, carbamic acid is unstable and will react with water molecules to form carbonate and ammonium ions (Yu et al., 2022). Nickel and calcium ions can be precipitated to form biocarbonate minerals by reacting with carbonate ions. Soybean-urease-based biocement can be applied to produce building materials and treat solid waste containing heavy metals.

4 Conclusions

This paper presents a new SUICP process that is similar to MICP technology and can be applied in the treatment of heavy metals and cementation of sandy soil. Soybean-based urease can be obtained by a water-soaking method for the production of biocement. Soybean powders mixed with DI water release urease into the aqueous solution and hydrolyze urea, thereby causing a change in conductivity. The optimal soaking time and soybean-powder concentration were 30 min and 130 g/L, respectively, and the average urease activity we obtained was bigger than 5 U. Soybean-based urease hydrolyzes urea to produce carbonate ions, which combine with nickel and calcium ions to form nickel carbonate and calcium carbonate, thereby reducing the concentration of cations. Under optimal conditions for removing nickel ions, the mass ratio of urea to nickel ions to SPF is 1:2.4:20. The removal efficiency also increases with higher concentrations of nickel ions and the optimal mass ratio. With regard to sandy soil, the UCS of sand blocks can be improved by soybean-urease-based biocement when the cementation level is higher than 3. We also found that the content of $CaCO_3$ in sand blocks increases at higher cementation levels. Thus, the SUICP technology could be used to consolidate heavy metal ions in solid waste, desert sands, and foundations of island reefs.

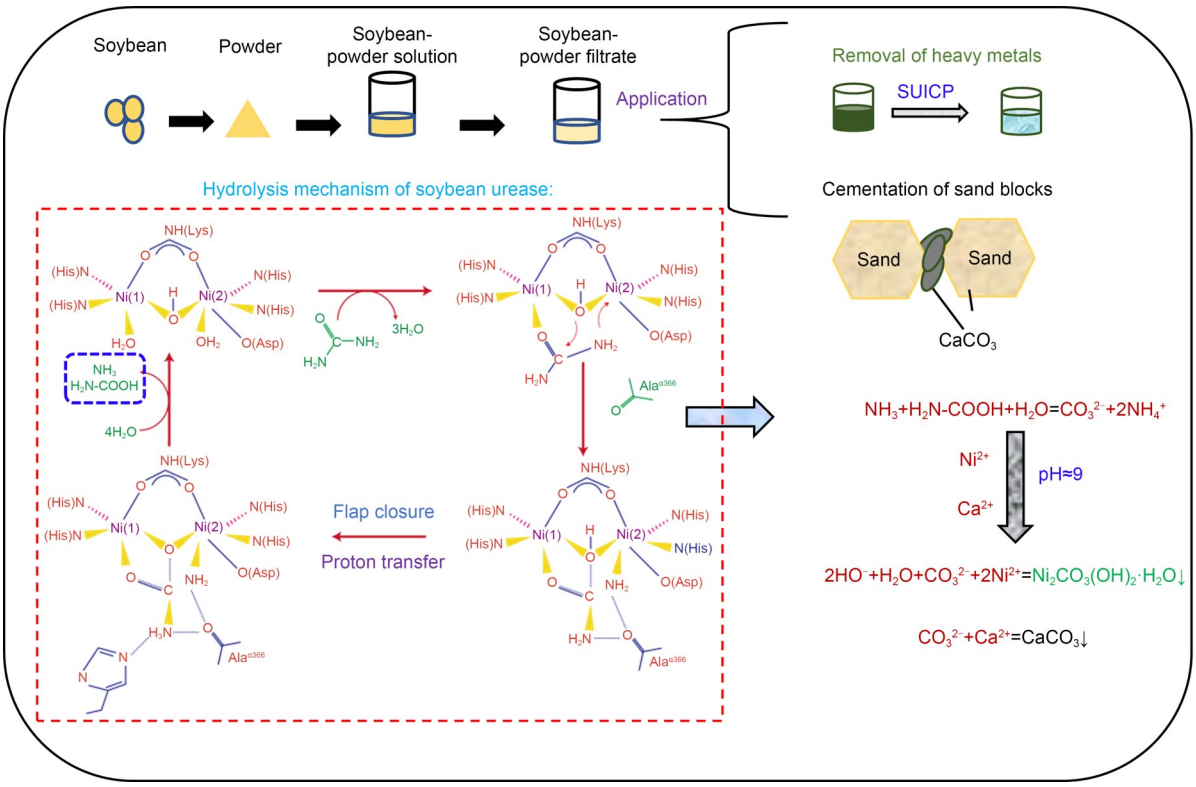

Fig. 8 Potential applications and formation mechanism of soybean-urease-based biocement. Reprinted from (Yu et al., 2022), Copyright 2022, with permission from Elsevier. Asp: aspartate; Ala: alanine; His: histidine; Lys: lysine

Acknowledgments

This work is supported by the Opening Funds of Jiangsu Key Laboratory of Construction Materials (No. CM2018-02), the Key Project of Natural Science Foundation of Zhejiang Province, China (No. LZ22E080003), and the General Project of Natural Science Foundation of Zhejiang Province, China (No. LY20E080002).

Author contributions

Xiaoniu YU performed the experiments and wrote the manuscript. Yidong XU reviewed and wrote the manuscript. Xiaoniu YU and Yidong XU edited and revised the final version.

Conflict of interest

Xiaoniu YU and Yidong XU declare that they have no conflict of interest.

References

Benini S, Rypniewski W, Wilson K, et al., 2001. Structure-based rationalization of urease inhibition by phosphate: novel insights into the enzyme mechanism. *JBIC Journal of Biological Inorganic Chemistry*, 6(8):778-790. https://doi.org/10.1007/s007750100254

Cheng L, Shahin MA, Cord-Ruwisch R, 2014. Bio-cementation of sandy soil using microbially induced carbonate precipitation for marine environments. *Géotechnique*, 64(12): 1010-1013. https://doi.org/10.1680/geot.14.T.025

Cheng L, Shahin MA, Mujah D, 2017. Influence of key environmental conditions on microbially induced cementation for soil stabilization. *Journal of Geotechnical and Geoenvironmental Engineering*, 143(1):04016083. https://doi.org/10.1061/(ASCE)GT.1943-5606.0001586

DeJong JT, Fritzges MB, Nüsslein K, 2006. Microbially induced cementation to control sand response to undrained shear. *Journal of Geotechnical and Geoenvironmental Engineering*, 132(11):1381-1392. https://doi.org/10.1061/(asce)1090-0241(2006)132:11(1381)

Do H, Wang YQ, Long ZH, et al., 2020. A psychrotolerant Ni-resistant *Bacillus cereus* D2 induces carbonate precipitation of nickel at low temperature. *Ecotoxicology and Environmental Safety*, 198:110672. https://doi.org/10.1016/j.ecoenv.2020.110672

Fan Q, Fan L, Quach WM, et al., 2023. Application of microbial mineralization technology for marine concrete crack repair: a review. *Journal of Building Engineering*, 69:106299. https://doi.org/10.1016/j.jobe.2023.106299

Fan YN, Du HX, Wei H, et al., 2022. Experimental study on urease activity and cementation characteristics of soybean. *Journal of Wuhan University of Technology-Materials Science Edition*, 37(4):636-644. https://doi.org/10.1007/s11595-022-2578-z

Gao YF, He J, Tang XY, et al., 2019. Calcium carbonate precipitation catalyzed by soybean urease as an improvement

method for fine-grained soil. *Soils and Foundations*, 59(5): 1631-1637. https://doi.org/10.1016/j.sandf.2019.03.014

Gao YQ, Hua C, Li YH, et al., 2022. Biological solutions for the remediation of cracks in ancient earthen structures: experimental studies. *Journal of Materials in Civil Engineering*, 34(11):04022312. https://doi.org/10.1061/(ASCE)MT.1943-5533.0004453

Garg R, Garg R, Eddy NO, 2023. Microbial induced calcite precipitation for self-healing of concrete: a review. *Journal of Sustainable Cement-Based Materials*, 12(3):317-330. https://doi.org/10.1080/21650373.2022.2054477

Gebru KA, Kidanemariam TG, Gebretinsae HK, 2021. Biocement production using microbially induced calcite precipitation (MICP) method: a review. *Chemical Engineering Science*, 238:116610. https://doi.org/10.1016/j.ces.2021.116610

He FJ, Chen JQ, 2013. Consumption of soybean, soy foods, soy isoflavones and breast cancer incidence: differences between Chinese women and women in western countries and possible mechanisms. *Food Science and Human Wellness*, 2(3-4):146-161. https://doi.org/10.1016/j.fshw.2013.08.002

Hoang T, Alleman J, Cetin B, et al., 2020. Engineering properties of biocementation coarse- and fine-grained sand catalyzed by bacterial cells and bacterial enzyme. *Journal of Materials in Civil Engineering*, 32(4):04020030. https://doi.org/10.1061/(ASCE)MT.1943-5533.0003083

Hoang T, Do H, Alleman J, et al., 2023. Comparative evaluation of freeze and thaw effect on strength of BEICP-stabilized silty sands and cement- and fly ash-stabilized soils. *Acta Geotechnica*, 18(2):1073-1092. https://doi.org/10.1007/s11440-022-01612-7

Jiang L, Jia GH, Wang YZ, et al., 2020. Optimization of sporulation and germination conditions of functional bacteria for concrete crack-healing and evaluation of their repair capacity. *ACS Applied Materials & Interfaces*, 12(9):10938-10948. https://doi.org/10.1021/acsami.9b21465

Jiang NJ, Liu R, Du YJ, et al., 2019. Microbial induced carbonate precipitation for immobilizing Pb contaminants: toxic effects on bacterial activity and immobilization efficiency. *Science of the Total Environment*, 672:722-731. https://doi.org/10.1016/j.scitotenv.2019.03.294

Kou HL, Wu CZ, Ni PP, et al., 2020. Assessment of erosion resistance of biocemented sandy slope subjected to wave actions. *Applied Ocean Research*, 105:102401. https://doi.org/10.1016/j.apor.2020.102401

Kou HL, Li ZD, Liu JH, et al., 2023. Effect of MICP-recycled shredded coconut coir (RSC) reinforcement on the mechanical behavior of calcareous sand for coastal engineering. *Applied Ocean Research*, 135:103564. https://doi.org/10.1016/j.apor.2023.103564

Lee S, Kim J, 2020. An experimental study on enzymatic-induced carbonate precipitation using yellow soybeans for soil stabilization. *KSCE Journal of Civil Engineering*, 24(7): 2026-2037. https://doi.org/10.1007/s12205-020-1659-9

Li L, Qian CX, Cheng L, et al., 2010. A laboratory investigation of microbe-inducing $CdCO_3$ precipitate treatment in Cd^{2+} contaminated soil. *Journal of Soils and Sediments*, 10(2):248-254. https://doi.org/10.1007/s11368-009-0089-6

Li Y, Wen KJ, Li L, et al., 2020. Experimental investigation on compression resistance of bio-bricks. *Construction and Building Materials*, 265:120751. https://doi.org/10.1016/j.conbuildmat.2020.120751

Lin H, Suleiman MT, Brown DG, 2020. Investigation of pore-scale $CaCO_3$ distributions and their effects on stiffness and permeability of sands treated by microbially induced carbonate precipitation (MICP). *Soils and Foundations*, 60(4):944-961. https://doi.org/10.1016/j.sandf.2020.07.003

Liu SH, Du K, Huang W, et al., 2021. Improvement of erosion-resistance of bio-bricks through fiber and multiple MICP treatments. *Construction and Building Materials*, 271: 121573. https://doi.org/10.1016/j.conbuildmat.2020.121573

Lv C, Tang CS, Zhu C, et al., 2022. Environmental dependence of microbially induced calcium carbonate crystal precipitations: experimental evidence and insights. *Journal of Geotechnical and Geoenvironmental Engineering*, 148(7): 04022050. https://doi.org/10.1061/(ASCE)GT.1943-5606.0002827

Meng H, Gao YF, He J, et al., 2021. Microbially induced carbonate precipitation for wind erosion control of desert soil: field-scale tests. *Geoderma*, 383:114723. https://doi.org/10.1016/j.geoderma.2020.114723

Moghal AAB, Lateef MA, Mohammed SAS, et al., 2020. Efficacy of enzymatically induced calcium carbonate precipitation in the retention of heavy metal ions. *Sustainability*, 12(17):7019. https://doi.org/10.3390/su12177019

Nile SH, Nile A, Oh JW, et al., 2020. Soybean processing waste: potential antioxidant, cytotoxic and enzyme inhibitory activities. *Food Bioscience*, 38:100778. https://doi.org/10.1016/j.fbio.2020.100778

Omoregie AI, Senian N, Li PY, et al., 2016. Ureolytic bacteria isolated from Sarawak limestone caves show high urease enzyme activity comparable to that of *Sporosarcina pasteurii* (DSM 33). *Malaysian Journal of Microbiology*, 12(6): 463-470.

Omoregie AI, Palombo EA, Ong DEL, et al., 2020. A feasible scale-up production of *Sporosarcina pasteurii* using custom-built stirred tank reactor for in-situ soil biocementation. *Biocatalysis and Agricultural Biotechnology*, 24:101544. https://doi.org/10.1016/j.bcab.2020.101544

Qian CX, Yu XN, Zheng TW, et al., 2022. Review on bacteria fixing CO_2 and bio-mineralization to enhance the performance of construction materials. *Journal of CO_2 Utilization*, 55:101849. https://doi.org/10.1016/j.jcou.2021.101849

Shu S, Yan BY, Ge B, et al., 2022. Factors affecting soybean crude urease extraction and biocementation via enzyme-induced carbonate precipitation (EICP) for soil improvement. *Energies*, 15(15):5566.

https://doi.org/10.3390/en15155566

Song MZ, Ju TY, Meng Y, et al., 2022. A review on the applications of microbially induced calcium carbonate precipitation in solid waste treatment and soil remediation. *Chemosphere*, 290:133229. https://doi.org/10.1016/j.chemosphere.2021.133229

Sun XH, Miao LC, Wu LY, et al., 2021. Theoretical quantification for cracks repair based on microbially induced carbonate precipitation (MICP) method. *Cement and Concrete Composites*, 118:103950. https://doi.org/10.1016/j.cemconcomp.2021.103950

Sun XH, Miao LC, Wang HX, et al., 2022. Sand foreshore slope stability and erosion mitigation based on microbiota and enzyme mix–induced carbonate precipitation. *Journal of Geotechnical and Geoenvironmental Engineering*, 148(8):04022058. https://doi.org/10.1061/(ASCE)GT.1943-5606.0002839

van der Bergh JM, Miljević B, Šovljanski O, et al., 2020. Preliminary approach to bio-based surface healing of structural repair cement mortars. *Construction and Building Materials*, 248:118557. https://doi.org/10.1016/j.conbuildmat.2020.118557

Whiffin VS, van Paassen LA, Harkes MP, 2007. Microbial carbonate precipitation as a soil improvement technique. *Geomicrobiology Journal*, 24(5):417-423. https://doi.org/10.1080/01490450701436505

Wu HR, Wu W, Liang WJ, et al., 2023. 3D DEM modeling of biocemented sand with fines as cementing agents. *International Journal for Numerical and Analytical Methods in Geomechanics*, 47(2):212-240. https://doi.org/10.1002/nag.3466

Wu MY, Hu XM, Zhang Q, et al., 2020. Application of bacterial spores coated by a green inorganic cementitious material for the self-healing of concrete cracks. *Cement and Concrete Composites*, 113:103718. https://doi.org/10.1016/j.cemconcomp.2020.103718

Xiao P, Liu HL, Xiao Y, et al., 2018. Liquefaction resistance of bio-cemented calcareous sand. *Soil Dynamics and Earthquake Engineering*, 107:9-19. https://doi.org/10.1016/j.soildyn.2018.01.008

Xiao Y, He X, Evans TM, et al., 2019. Unconfined compressive and splitting tensile strength of basalt fiber–reinforced biocemented sand. *Journal of Geotechnical and Geoenvironmental Engineering*, 145(9):04019048. https://doi.org/10.1061/(ASCE)GT.1943-5606.0002108

Xiao Y, Zhang ZC, Stuedlein AW, et al., 2021. Liquefaction modeling for biocemented calcareous sand. *Journal of Geotechnical and Geoenvironmental Engineering*, 147(12):04021149. https://doi.org/10.1061/(ASCE)GT.1943-5606.0002666

Xiao Y, Ma GL, Wu HR, et al., 2022. Rainfall-induced erosion of biocemented graded slopes. *International Journal of Geomechanics*, 22(1):04021256. https://doi.org/10.1061/(ASCE)GM.1943-5622.0002239

Xiao Y, Xiao WT, Wu HR, et al., 2023. Fracture of interparticle MICP bonds under compression. *International Journal of Geomechanics*, 23(3):04022316. https://doi.org/10.1061/IJGNAI.GMENG-8282

Xue ZF, Cheng WC, Wang L, et al., 2022. Effects of bacterial inoculation and calcium source on microbial-induced carbonate precipitation for lead remediation. *Journal of Hazardous Materials*, 426:128090. https://doi.org/10.1016/j.jhazmat.2021.128090

Yi HH, Zheng TW, Jia ZR, et al., 2021. Study on the influencing factors and mechanism of calcium carbonate precipitation induced by urease bacteria. *Journal of Crystal Growth*, 564:126113. https://doi.org/10.1016/j.jcrysgro.2021.126113

Yin TT, Lin H, Dong YB, et al., 2021. A novel constructed carbonate-mineralized functional bacterial consortium for high-efficiency cadmium biomineralization. *Journal of Hazardous Materials*, 401:123269. https://doi.org/10.1016/j.jhazmat.2020.123269

Yu XN, Jiang JG, 2019. Phosphate microbial mineralization removes nickel ions from electroplating wastewater. *Journal of Environmental Management*, 245:447-453. https://doi.org/10.1016/j.jenvman.2019.05.091

Yu XN, Rong H, 2022. Seawater based MICP cements two/one-phase cemented sand blocks. *Applied Ocean Research*, 118:102972. https://doi.org/10.1016/j.apor.2021.102972

Yu XN, Pan XH, 2023. One-phase improvement of sandy soil using seawater-based soybean-induced carbonate precipitation. *Journal of Sustainable Cement-Based Materials*, 12(8):962-971. https://doi.org/10.1080/21650373.2022.2142985

Yu XN, Zhang ZH, 2023a. Calcium carbide sludge activated fly ash mixture for offshore construction and its crack repair using seawater-mixed bioslurry cement. *Journal of Cleaner Production*, 395:136456. https://doi.org/10.1016/j.jclepro.2023.136456

Yu XN, Zhang QY, 2023b. Microbially/CO_2-derived $CaCO_3$ cement and its microstructural and mechanical performance. *Journal of Sustainable Cement-Based Materials*, 12(9):1156-1168. https://doi.org/10.1080/21650373.2023.2178539

Yu XN, Yang HQ, Wang H, 2022. A cleaner biocementation method of soil via microbially induced struvite precipitation: a experimental and numerical analysis. *Journal of Environmental Management*, 316:115280. https://doi.org/10.1016/j.jenvman.2022.115280

Zhang D, Shahin MA, Yang Y, et al., 2022. Effect of microbially induced calcite precipitation treatment on the bonding properties of steel fiber in ultra-high performance concrete. *Journal of Building Engineering*, 50:104132. https://doi.org/10.1016/j.jobe.2022.104132

Electronic supplementary materials

Tables S1–S7, Figs. S1–S5